# Living Materials Constructed with Dynamic Covalent Interface between Synthetic Polymers and *B. subtilis*

Hyuna Jo[1] and Seunghyun Sim[1,2,3] *

[1]*Department of Chemistry, University of California Irvine, Irvine, California 92697, United States*

[2]*Department of Chemical and Biomolecular Engineering, University of California Irvine, Irvine, California 92697, United States*

[3]*Department of Biomedical Engineering, University of California Irvine, Irvine, California 92697, United States*

**ABSTRACT**

With advances in the field of synthetic biology increasingly allowing us to engineer living cells to perform intricate tasks, incorporating these engineered cells into the design of synthetic polymeric materials will enable programming materials with a wide range of biological functionalities. However, employable strategies for the design of synthetic polymers that form a well-defined interface with living cells and seamlessly integrate their functionalities in materials are still largely limited. Herein, we report the first example of living materials constructed with a dynamic covalent interface between synthetic polymers and living *B. subtilis* cells. We showed

that 3-acetamidophenylboronic acid (APBA) and polymers of APBA (pAPBA) form dynamic covalent bonds with available diols on the *B. subtilis* cell surface. Importantly, pAPBA binding to *B. subtilis* shows a multivalent effect with complete reversibility upon addition of competitive diol species, such as fructose and sorbitol. On the basis of these findings, we constructed telechelic block copolymers with pAPBA chain ends that crosslink *B. subtilis* cells and produced self-standing living materials. We further demonstrated that the encapsulated cells could be retrieved upon immersing these materials in solutions containing competitive diols and further subjected to biological analyses. This work establishes the groundwork for building a myriad of synthetic polymeric materials integrating engineered living cells and provides a platform for understanding the biology of cells confined within materials.

## INTRODUCTION

Natural biological materials – such as wood, bone, and skin – comprise living cells and macromolecular scaffolds. As shown in these examples, the seamless integration of living cells into a structural scaffold enables complex biological tasks that are not possible with purely synthetic materials or cells alone. For example, we see this in bone as it provides structural support, serves as a mineral reservoir, and produces red blood cells, all at the same time.[1] With advances in the field of synthetic biology increasingly allowing us to engineer living cells to perform intricate tasks, incorporating engineered living cells into the design of polymeric materials will enable high-performance polymeric materials equipped with a wide range of biological functionalities. In particular, *Bacillus subtilis* offers unique advantages as a building block for engineered living materials: It is genetically tractable, exhibits extraordinary secretion capacity, lacks toxic byproducts, and survives harsh environments by forming dormant spores.[2] Motivated by these

characteristics, recent studies have exploited biologically-derived macromolecules for producing living materials with *B. subtilis*. For example, Voigt and colleagues demonstrated 3-dimensional printing of agarose hydrogels containing engineered *B. subtilis* spores.[3] Zhong and co-workers showcased printable living materials based on *B. subtilis* biofilms, which can be manipulated by bacterial amyloid TasA production.[4]

These living materials, in essence, are composite materials comprising at least two different physical and chemical components: polymers and living cells. Therefore, their mechanical and dynamic properties should strongly depend on the molecular composition of the interface. However, bottom-up strategies for the design of synthetic polymers that form a well-defined interface with living cells and seamlessly integrate living functionalities in materials are still largely limited. In addition, there is a significant knowledge gap in understanding the biology of cells confined in materials due to the lack of a platform allowing both spatial confinement and on-demand release of cells for biological analysis. Taken together, the ideal interface between polymeric materials and living cells should be molecularly well-defined, provide sufficient connection and collective bond strength for seamless integration, and provide means to capture and release encased cells reversibly. Dynamic covalent chemistries have attracted significant attention as a strategy for developing polymeric materials that are adaptable, stimuli-responsive, and self-healing.[5-12] Among these dynamic covalent systems, boronic acids form dynamic covalent bonds with 1,2- or 1,3-diol species and undergo rapid exchange when competing diols are present at ambient conditions in aqueous media.[7-11] Therefore, utilizing boronic ester-mediated covalent bond formation in building the cell-material interface is expected to yield adaptive and dynamic living materials.

Here, we report living materials constructed with a dynamic covalent interface between synthetic polymers and living *B. subtilis* cells. We demonstrated that 3-acetamidophenylboronic acid (APBA) and polymers containing APBA repeating units (pAPBA) form dynamic covalent bonds with diols on the *B. subtilis* cell surface. In addition, we observed a multivalent effect in pAPBA binding to *B. subtilis* with complete reversibility when competitive diol species are present. Telechelic block copolymers with pAPBA chain ends (pAPBA–$PEG_x$–pAPBA), designed and synthesized based on these findings, crosslink *B. subtilis* cells and yield stable self-standing living materials in a hydrogel form. As these materials are constructed by dynamic covalent interface, encapsulated cells could be retrieved upon immersing these materials in solutions containing competitive diols and further subjected to biological analyses.

## RESULTS AND DISCUSSION

### 3-Acetamidophenylboronic acid (APBA) binds to *B. subtilis* cell surface.

*B. subtilis* is a gram-positive organism with a peptidoglycan cell wall. The cell surface of *B. subtilis* comprises a disordered mesh of crosslinked peptidoglycan and teichoic acids.[13] Teichoic acids are anionic polymers with glycerol phosphate or ribitol phosphate backbone.[14] There are two different types of teichoic acids; wall teichoic acid and lipid teichoic acid. Wall teichoic acids are covalently linked to the N-acetylmuramic acid residues of peptidoglycan, and lipid teichoic acids have a lipid anchor which is embedded in the outer leaflet of the cell membrane. The hydroxyl groups in the main chain of teichoic acids are modified with D-alanine or glucose. We hypothesized that APBA would form dynamic covalent bonds with available 1,2-*cis* diols on *B. subtilis*, including glucose side chains in surface teichoic acids (Figure 1a), and set out to test this hypothesis. A fluorescent probe with the APBA motif, APBA-sCy5, was synthesized by a reaction

of sulfo-cyanine 5 (sCy5) NHS esters and 3-aminophenylboronic acid in the presence of triethylamine for 16 h (Figure 1b, Figure S1). We also prepared a control probe molecule carrying a trisaminomethane (Tris) group instead of the APBA unit, Tris-sCy5 (Figure 1b, Figure S2). Phosphate buffered saline (PBS; 20 mM, pH 7.4) suspensions of wild type (PY79 laboratory strain, abbreviated as WT) *B. subtilis* cells are treated with a PBS solution of APBA-sCy5 (15 $\mu$M) or Tris-sCy5 (15 $\mu$M) at 25 °C for 3 hours. After washing with PBS, the cell suspensions were subjected to fluorescence microscopy ($\lambda_{ex}$ = 630 nm). As shown in Figure 1c, a strong fluorescence emission on the cell surface was observed when they were treated with APBA-sCy5, whereas cells treated with Tris-sCy5 did not show appreciable fluorescence in the same setting (Figure 1d). Fluorescence spectroscopy ($\lambda_{ex}$ = 630 nm) of these solutions revealed that the cell suspensions treated with APBA-sCy5 were 9-fold more emissive than those treated with Tris-sCy5 (Figure 1g).

In an effort to molecularly understand the binding behavior of APBA-sCy5 on the cell surface of *B. subtilis*, we utilized a *tagE*-deletion mutant. The *tagE* gene encodes a glycosyltransferase that is responsible for wall teichoic acid glycosylation, and deletion of this gene results in the loss of glucose side chains in the poly(glycerol phosphate) backbone.[15] When *B. subtilis tagE*-deletion mutant (ΔtagE) was treated with APBA-sCy5, fluorescence localization on the cell surface was similar to that of WT *B. subtilis* cells, but was of lower intensity on the cell surface (Figure 1e). The bulk fluorescence measurement of the cell suspension corresponded with this observation, resulting in 57% lower total fluorescence than that of the WT *B. subtilis* (Figure 1g). This result suggests that glucose side chains on wall teichoic acid serve as one of the major binding sites for APBA. We speculate that terminal diols at the chain end of teichoic acid are another likely binding site of APBA. The molecular composition of the cell surface of gram-negative bacteria such as *E. coli* is distinct from gram-positive bacteria, as they have outer phospholipid membranes decorated

with membrane proteins and lipopolysaccharide. Interestingly, a PBS suspension of *E. coli* (laboratory strain) treated with APBA-sCy5 did not show appreciable surface labeling (Figure S19).

**Polymers with APBA repeating units bind to *B. subtilis* cell surface and exhibit a multivalent effect.**

Upon confirming the binding affinity of APBA to *B. subtilis* cell surface, we set out to synthesize APBA-containing polymers to understand the nature of the interaction between *B. subtilis* cell surface with macromolecules containing APBA motif. Fluorescently labeled poly(APBA) molecules, $pAPBA_n$-sCy5 were synthesized through reversible addition-fragmentation chain-transfer polymerization (RAFT) (Figure 2a).[16] The terminal chain transfer groups on the polymers were cleaved by butylamine for subsequent conjugation of maleimide-sCy5 with the thiol groups at the chain termini.[17] Gel permeation chromatography (GPC, Figure 2b) of the reaction mixture showed polymers having 40 ($pAPBA_{40}$-sCy5, Figure 2b, gray), 50 ($pAPBA_{50}$-sCy5, Figure 2b, blue), and 62 ($pAPBA_{62}$-sCy5, Figure2b, red) APBA repeating units, which was in a reasonable agreement to the $^1$H NMR results (Figure S3–8).

*B. subtilis* cell suspensions were mixed with $pAPBA_n$-sCy5 (15 $\mu$M), and the resulting suspension (PBS 20 mM, pH 7.4, 5% MeOH), after incubation for 3 h, was washed with PBS. The cell samples were subjected to fluorescence microscopy analysis and bulk fluorescence measurement. As shown in Figure 2g–i, fluorescence microscopy visualized the localization of $pAPBA_n$-sCy5 on the cell surface. However, distinct from the small molecule probe APBA-sCy5, fluorescent puncta were detected from the bound $pAPBA_{40}$-sCy5 (Figure 2d and 2g) and $pAPBA_{50}$-sCy5 (Figure 2e and 2h) to the cells, presumably due to the entangled polymer chains in local areas

of the cell surface. Corroborating this result, hydrodynamic sizes detected from the dynamic light scattering analysis of PBS solution of the polymers (15 $\mu$M) indicated that pAPBA$_n$-sCy5 polymers exist in aggregated forms in aqueous solutions (Figure S18). Interestingly, mixtures of pAPBA$_{62}$-sCy5 and *B. subtilis* cells yielded various sizes of cellular aggregates that colocalize with strong fluorescence from the fluorescently labeled polymer (Figure 2f and 2i). This result suggests that a long chain of pAPBA$_{62}$ serves as an intracellular crosslinking agent by providing binding sites for more than one cell (Figure 2c). The numbers of bound pAPBA$_n$-sCy5 to the cells were evaluated based on bulk fluorescence measurements of the labeled, washed, and resuspended cell suspensions (Figure 2j and Figure S23–26). The intensity values are normalized by the colony-forming unit (CFU) of the cell suspension used for each sample prior to the polymer treatment. The estimated average number of polymer molecules per one *B. subtilis* cell increases with the number of the repeating units in pAPBA$_n$-sCy5. We speculate that aggregation behaviors of pAPBA$_n$-sCy5 may be the reason for the observed multivalent effect in binding affinity to the cell. In addition, since one of the primary binding sites of the APBA to *B. subtilis* cell surface is the glucose side chains in wall teichoic acid, the multivalent effect in pAPBA binding to the *B. subtilis* surface may be due to the bi-dentate bridge of two adjacent APBA units binding to one glucose molecule in the furanose form via 1,2- and 5,6-*cis*-diols.[18-20]

The estimated average number of the monomeric fluorescent probe, APBA-sCy5, on the cell surface was larger than that of the smallest polymer chain, pAPBA$_{40}$-sCy5. Considering the peptidoglycan mesh structure of the *B. subtilis* cell surface and the relative hydrodynamic volume of the aggregated polymers (Figure S18), we speculate that the polymers, pAPBA$_n$-sCy5, are more likely to interact with the exposed diol motifs on the cell surface, whereas the small molecule probe

APBA-sCy5 is more likely to penetrate the peptidoglycan mesh structure and label the inner part of the cell wall.

**Polymers with APBA repeating units detach from to *B. subtilis* cell surface upon addition of competitive diols.**

Upon adding exogenous diol species, boronate esters can undergo competitive exchange reactions (Figure 3a). Based on this mechanism, we investigated whether the cell-bound small molecule APBA probe (APBA-sCy5) and APBA containing polymers ($pAPBA_n$-sCy5; n = 40, 50, and 62) could be detached in the presence of exogenous diols by fluorescence microscopy analysis and bulk fluorescence measurements. In brief, we supplemented selected diols (50 mM) in PBS (20 mM, pH 7.4) suspension of labeled cells (Figure 1c and 2g–i). The mixture was agitated (800 rpm) at 30 °C, washed with PBS, and then subjected to fluorescence microscopy ($\lambda_{ex}$ = 630 nm) and bulk fluorescence measurement. After 6 hours of incubation with fructose, the fluorescence on the cell surface was diminished in mixtures of $pAPBA_n$-sCy5 molecules and *B. subtilis*, indicating that the polymers bound to the cell surface were readily detached upon competitive diol exchange at the boronate ester linkage (Figure 3e–g). Noteworthy is that the large cellular aggregates observed in the mixture of $pAPBA_{62}$-sCy5 and *B. subtilis* were completely dissociated into single cells (Figure 3d and 3g) upon fructose treatment. This change was accompanied by a near-complete diminishment of the fluorescence signal on the cell surface. The bulk fluorescence measurements of these mixtures (Figure 3i–k and Figure S27–30) showed a greater than 90% reduction in fluorescence intensity upon addition of fructose compared to the initial point and supported our observations in fluorescence microscopy. We also found that common monosaccharides, glucose and sorbitol (50 mM each), could exert a similar effect to the bound

pAPBA$_n$-sCy5 polymers to the cells, evidenced by decrements in fluorescent intensity on the cell surface (Figures S20–21) as well as in bulk fluorescence measurements (Figure 3i–k and Figure S27–30). The generally observed sugar reversibility of pAPBA$_n$-sCy5/cell complexes follows the order of fructose ≈ sorbitol > glucose. Since both glucose and fructose can exist in furanose and pyranose forms,[21] fructose shows a higher binding affinity to phenylboronic acid species than glucose because the highest binding affinity isomer, β-D-fructofuranose, amounts to 25% of the total fructose in an ambient condition.[22-23] In contrast, the highest binding affinity form of glucose is only 0.14% of the total glucose. The apparent association constants of APBA determined by Sumerlin and colleagues are 350 $M^{-1}$ for fructose, 610 $M^{-1}$ for sorbitol, and 8.1 $M^{-1}$ for glucose.[24] Our results show fructose is similar to or slightly more effective than sorbitol in detaching bound pAPBA-sCy5 from *B. subtilis* surface, which may be due to the macromolecular nature of pAPBA$_n$-sCy5 and teichoic acids on the cell surface. It is also worthwhile to note that *B. subtilis* uses glucose as the primary carbon source for its metabolism.[25-26] When glucose is added to the pAPBA$_n$-sCy5/cell complex (Figure 3i–k and Figure S20), the fluorescence from the cell surface after 6 hours of incubation was higher than that of the 3-hour incubation. This result hints that the externally added glucose gets consumed by cells over time. Contrasting to the results of pAPBA$_n$-sCy5, in the case of the bound monomeric APBA molecule (APBA-sCy5) to the cell, adding exogenous diols did not significantly reduce the fluorescence (Figure 3h). This result corroborates our earlier speculation that APBA-sCy5 is more likely to penetrate the peptidoglycan mesh structure and label the inner part of the peptidoglycan cell wall. Even with the same APBA binding motif, the bound polymers would be readily detached because their binding sites are more exposed to the surface. On the other hand, dissociation of the bound APBA-sCy5 residing deeper in the peptidoglycan network would experience more physical barriers to this exchange reaction.

**Telechelic polymers with pAPBA chain end yield self-standing hydrogel upon mixing with *B. subtilis*.**

On the basis of our findings that APBA-containing synthetic macromolecules form a dynamic covalent interface with *B. subtilis* cell, we synthesized telechelic polymers having hydrophilic polyethylene glycol (PEG) mid-block and pAPBA end blocks, pAPBA–$PEG_x$–pAPBA (Figure 4a; x refers to molecular weights of the mid-block), and varied the mid-block PEG molecular weight from 4,000 g/mol to 20,000 g/mol. Since the mid-block PEG is known to swell in an aqueous environment, this telechelic design was expected to yield macroscopic soft materials crosslinking *B. subtilis* cells (Figure 4b). Gel permeation chromatography (GPC, Figure 4c) of the reaction mixture showed curves corresponding to molecular weights of 9,369 g/mol for pAPBA–$PEG_{4k}$–pAPBA, 16,740 g/mol for pAPBA–$PEG_{10k}$–pAPBA, and 27,928 g/mol for pAPBA–$PEG_{20k}$–pAPBA (Table 1). Based on these results, the total degree of polymerization at the chain ends were 30 (15 for each end), 38 (19 for each end), 44 (22 for each end) for pAPBA–$PEG_{4k}$–pAPBA, pAPBA–$PEG_{10k}$–pAPBA, and pAPBA–$PEG_{20k}$–pAPBA, respectively. These results were in a reasonable agreement to the $^1$H NMR results (Figure S12–17). Adding a PBS (20 mM, pH 7.4) suspension of *B. subtilis* cells ($5.0 \times 10^{10}$ cells/mL) to a PBS solution (80 mM, pH 9.4) of pAPBA–$PEG_x$–pAPBA polymers (Figure 4d; see supplementary methods) yields self-standing hydrogels (Figure 4e and 4f), confirming our expectation of creating a 3-dimensional network of living cells and telechelic polymers. We note that preparation of the high concentration of the pAPBA–$PEG_x$–pAPBA polymers (> 3 wt%) in a PBS buffer is important for gelation. If a polymer solution of 3 wt% (or less) is used, it results in a turbid suspension. In Figure 4g, characteristic linear rheological measurements of a PBS solution of pAPBA–$PEG_{4k}$–pAPBA (5 wt%) in the presence and absence of *B. subtilis* cells ($5.0 \times 10^{10}$ cells/mL) are presented (25 °C, see supplementary methods). Adding

cells to the pAPBA–$PEG_{4k}$–pAPBA solutions resulted in a few orders of magnitude increase in storage moduli. These results strongly indicate that the dynamic covalent bond formation between pAPBA and the cell surface is the driving force for gelation, and *B. subtilis* cells served as a crosslinker for this hydrogel network. Similar trends were observed when solutions of pAPBA–$PEG_{10k}$–pAPBA and pAPBA–$PEG_{20k}$–pAPBA were mixed with cell suspensions (Figure S32). These living materials exhibited larger storage moduli than the loss moduli over the entire range of frequencies examined (Figure 4h). Telechelic polymers containing a larger PEG mid-block would have a lower concentration of chains per unit volume at a given mass concentration. Similar to the rheological behavior of associative telechelic protein hydrogels reported by Tirrell and co-workers,[27] the magnitude of the plateau storage moduli of these living materials decreases with the increasing mid-block size (Figure 4h). Macroscopically, these hydrogels are self-standing, hold their shape, and are moldable. As shown in Figures 4k and 4l, they can be easily fabricated and molded into desired shapes and sizes. Harnessing engineered *B. subtilis* cells constitutively expressing red fluorescent protein, we prepared living materials (Figure 4i–l) showing red fluorescence (Figure 4j–l; $\lambda_{ex}$ = 630 nm).

**_B. subtilis_ cells encased in polymeric living material can be retrieved and analyzed upon exposure to competitive diol species.**

We set out to investigate whether encased cells in these living materials could be retrieved upon immersing the materials into solutions containing fructose by the diol-exchange reaction at APBA binding sites (Figure 5a). If encased living cells could be retrieved from materials and subjected to biological analysis, it opens a new possibility of understanding how immobilized living cells are biologically different from the cells grown in liquid culture. Living materials, which were

prepared by mixing a PBS solution of pAPBA–$PEG_{4k}$–pAPBA (5 wt%) and a suspension of *B. subtilis* cells ($5.0 \times 10^{10}$ cells/mL), were immersed in a known volume of PBS (20 mM, pH 7.4) in the absence (Figure 5b–d, left) and presence (Figure 5b–d, right) of fructose (100 mM) and were mechanically agitated (200 rpm) at 30 °C for 16 hours. In just 30 minutes, the supernatant of the materials treated with fructose turned opaque, indicating the release of the encased cells (Figure 5c, right). After 16 hours, the materials immersed in fructose solution were completely dissolved, whereas the materials immersed in PBS without fructose remained as swollen networks of polymers and living cells. After confirming that cells cannot divide in the fructose solution (Figure S33), we quantified the absorbance of the resulting supernatant at 600 nm ($OD_{600}$). Since cell division is not possible in the fructose solution as it is lacking key nitrogen sources for cellular growth, the absorbance reading should directly reflect the number of cells that become freed from the polymeric network. We observed a gradual increase in $OD_{600}$ in both cases, but the $OD_{600}$ values of the PBS solution that contains fructose were significantly higher than that of the PBS solution without fructose (Figure 5e). We prepared a control solution containing the same total amount of cells that were supposed to be in living materials in the same volume of the PBS solution to quantitatively compare the number of cells freed from the scaffold (Figure 5e, gray bar). Assuming $OD_{600}$ intensities in this range have a linear relationship to the number of cells, 65% of cells were retrieved from this hydrogel upon the fructose treatment. We investigated the cell viability of the retrieved cells using a 5-cyano-2,3-ditolyl tetrazolium chloride (CTC) reagent, which has been used to estimate the respiratory activity of the bacterial cells. Metabolically active cells with functional electron transport chains are expected to reduce CTC, resulting in insoluble and red fluorescent formazan ($\lambda_{ex}$ = 450 nm). Retrieved cells (1 mL) from the living materials were incubated with an aqueous solution of CTC (50 mM, 100 $\mu$L) for 30 min at 37 °C and washed with

PBS before being subjected to the fluorescence spectrometry (Figure S31). The control cell samples containing the same number of cells, based on $OD_{600}$, are directly collected from the saturated bacterial cell culture. As shown in Figure 5f, the cell released from the hydrogel showed similar metabolic activity (88%) compared to the control. Further, we prepared living materials with engineered *B. subtilis* constitutively expressing RFP when in the vegetative state. The RFP fluorescence intensities from suspensions containing retrieved cells were comparable to that of the control, which contained the same cells directly from overnight cultures (Figure S22).

## CONCLUSION

In conclusion, we report living materials constructed with a dynamic covalent interface between pAPBA-containing synthetic polymers and living *B. subtilis* cells, which to the best of our knowledge is unprecedented. This development was made possible by our finding that 3-acetamidophenylboronic acid (APBA) and polymers of APBA (pAPBA) form dynamic covalent bonds with available diols on the *B. subtilis* cell surface, and pAPBA binding to *B. subtilis* shows a multivalent effect with complete reversibility upon adding competitive diol species. Given the rapidly-growing toolbox of synthetic biology and expanding interest in its use in addressing challenges in medicine, sensing, sustainability, and defense, we envision this work will expand the scope of functional biomaterials by opening possibilities for integrating emergent cellular functionalities into the design of high-performance polymeric materials. In addition, due to the dynamic covalent interface, the living cells encased in these materials can be retrieved upon exposure to solutions containing competitive diol species, allowing us to perform detailed biological analyses. In this regard, this work also establishes the critical groundwork of a future

platform we envision for understanding the biology of cells confined within materials by allowing transcriptomic or proteomic analyses.

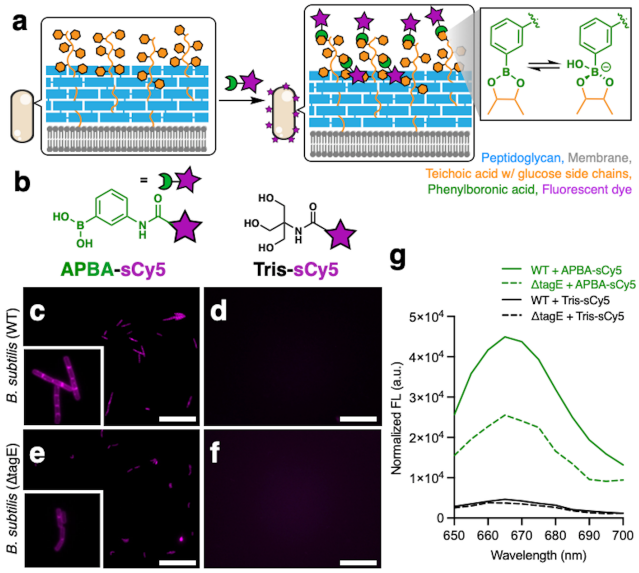


**Figure 1. 3-Acetamidophenylboronic acid (APBA) binds to *B. subtilis* cell surface.** (a) Schematic illustration of the binding of APBA-sCy5, bearing APBA motif and a fluorescent dye sulfo-cyanine 5 (sCy5), to glucose side chains of the wall teichoic acids on the surface of *B. subtilis*. (b) Molecular structures of APBA-sCy5 and Tris-sCy5. (c–f) Representative fluorescence microscope ($\lambda_{ex}$ = 630 nm, $\lambda_{obs}$ = 690–740 nm) images of wild type (PY79 laboratory strain, abbreviated as WT) and *tagE*-deletion mutant (ΔtagE) *B. subtilis* cells after 3-hour incubation at room temperature with fluorescent probes. (c) APBA-sCy5 with WT, (d) Tris-sCy5 with WT, (e) APBA-sCy5 with ΔtagE, and (f) Tris-sCy5 with ΔtagE. The cells were incubated with a fluorescent probe (15 $\mu$M) in PBS (20 mM, pH 7.4) and washed with PBS twice. Scale bars = 50 $\mu$m. (g) Fluorescence spectra ($\lambda_{ex}$ = 630 nm) of WT (solid lines) and ΔtagE (dotted lines) *B. subtilis* cells after 3-hour incubation at room temperature in PBS with APBA-sCy5 (green) and Tris-sCy5 (black). The cells were incubated with a fluorescent probe (15 $\mu$M) in PBS (20 mM, pH 7.4) and washed with PBS twice. The fluorescence intensities were normalized to the optical density (absorbance at 600 nm) of each cell suspension.

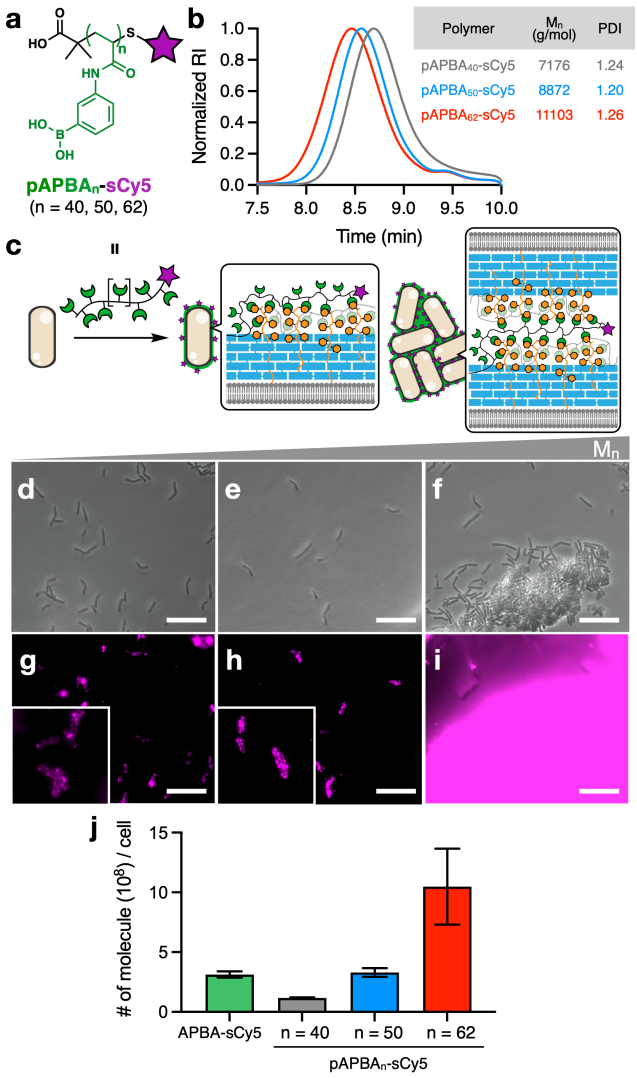


**Figure 2. Polymers with APBA repeating units bind to *B. subtilis* cell surface and show a multivalent effect.** (a) Molecular structure of polymers pAPBA$_n$-sCy5 (n = 40, 50, and 62). (b) Gel permeation chromatography (GPC) of pAPBA$_n$-sCy5 in DMF and a summary of experimental molecular weight and polydispersity index (PDI) based on the GPC data. (c) Schematic illustration of the binding behaviors of pAPBA$_n$-sCy5 to the *B. subtilis* cell surface. With the increasing number of the APBA repeating units, *B. subtilis* cells tend to form large cellular aggregates. (d–i) Bright-field and fluorescence microscope images ($\lambda_{ex}$ = 630 nm, $\lambda_{obs}$ = 690–740 nm) of *B. subtilis* cells incubated with pAPBA$_n$-sCy5. The upper panel shows representative bright-field images, and the lower panel represents fluorescence microscope images corresponding to them. (d & g) pAPBA$_{40}$-sCy5, (e & h) pAPBA$_{50}$-sCy5, and (f & i) pAPBA$_{62}$-sCy5. The cells were incubated for 3 hours with pAPBA$_n$-sCy5 (15 $\mu$M) in PBS (20 mM, pH 7.4) and washed with PBS twice. Scale bars = 50 $\mu$m. (j) Average number of APBA-sCy5 (green), pAPBA$_{40}$-sCy5 (gray), pAPBA$_{50}$-sCy5 (blue), and pAPBA$_{62}$-sCy5 (red) molecules per one *B. subtilis* cell. These values were calculated from the bulk fluorescence intensity and colony-forming unit of each cell suspension. $N$ = 3 (biological replicates). Error bars represent ± s.e.m.

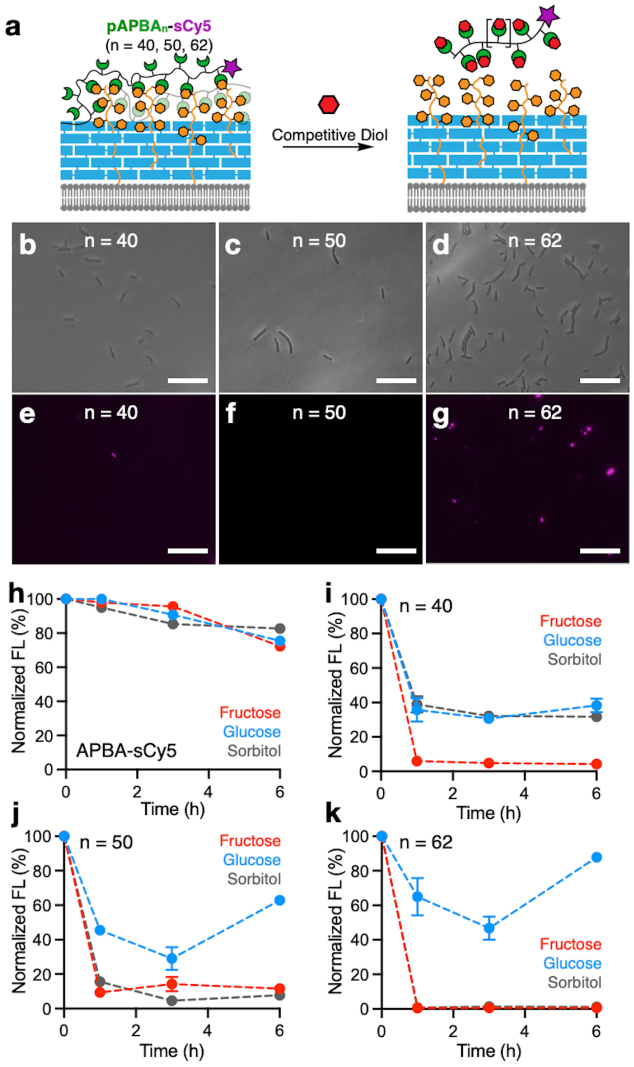


**Figure 3. Polymers with APBA repeating units detach from to *B. subtilis* cell surface upon addition of competitive diols.** (a) Schematic illustration of pAPBA$_n$-sCy5 dissociating from the surface of *B. subtilis* cells in the presence of competing diols. (d–i) Bright-field and fluorescence microscope images ($\lambda_{ex}$ = 630 nm, $\lambda_{obs}$ = 690–740 nm) of *B. subtilis* cells incubated with pAPBA$_n$-sCy5 for 3 hours, washed, and subsequently treated with fructose (50 mM) in PBS (20 mM, pH 7.4) for 6 hours. The upper panel shows representative bright-field images, and the lower panel represents fluorescence microscope images corresponding to them. (b & e) pAPBA$_{40}$-sCy5, (c & f) pAPBA$_{50}$-sCy5, and (d & g) pAPBA$_{62}$-sCy5. The cells were washed with PBS twice. Scale bars = 50 $\mu$m. (h–k) Normalized fluorescence profiles of *B. subtilis* cell suspension first incubated with (h) APBA-sCy5, (i) pAPBA$_{40}$-sCy5, (j) pAPBA$_{50}$-sCy5, or (k) pAPBA$_{62}$-sCy5 for 3 hours and subsequently treated with competing diols over 6 hours. $N$ = 3 (biological replicates). Error bars represent ± s.e.m.

**Table 1. Telechelic polymers containing pAPBA end-blocks**

| Polymer | End-block | Mid-block | $M_n$ (g/mol) | PDI |
|---|---|---|---|---|
| pAPBA–$PEG_{4k}$–pAPBA | 2n = 30 | PEG 4000 | 9369 | 1.48 |
| pAPBA–$PEG_{10k}$–pAPBA | 2n = 38 | PEG 10000 | 16740 | 1.31 |
| pAPBA–$PEG_{20k}$–pAPBA | 2n = 44 | PEG 20000 | 27928 | 1.67 |

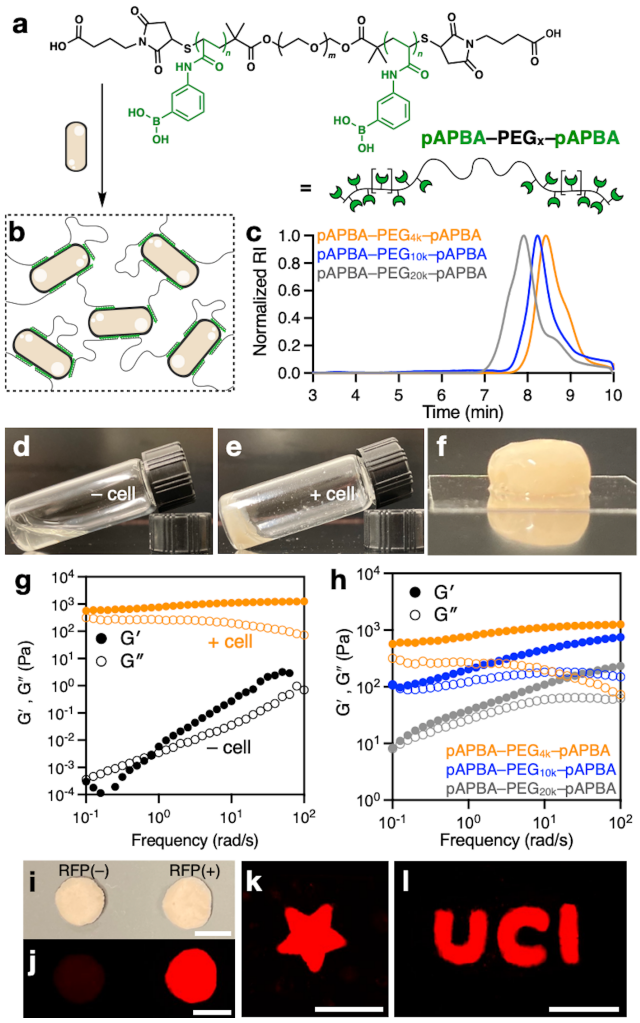


**Figure 4. Telechelic polymers with pAPBA chain end yield self-standing hydrogel upon mixing with *B. subtilis*.** (a) Molecular structure of telechelic block polymers pAPBA-PEG$_x$-pAPBA bearing a polyethylene glycols mid-block (molecular weight: 4,000, 10,000, and 20,000 g/mol) and pAPBA end blocks at each end. (b) Proposed mechanism for network formation in living materials. (c) GPC of pAPBA-PEG$_x$-pAPBA in DMF. (d–e) Optical images of a PBS buffer (80 mM, pH 9.4) solution of pAPBA-PEG$_{4k}$-pAPBA in the (d) absence and (e) presence of *B. subtilis* ($5.0 \times 10^{10}$ cells/mL). (f) An optical image of a self-standing hydrogel made with pAPBA-PEG$_{4k}$-pAPBA and *B. subtilis* cells. (g) Storage moduli G′ (filled circle) and loss moduli G″ (open circle) of pAPBA-PEG$_{4k}$-pAPBA in the absence (black, strain = 50%) and the presence (orange, strain = 1%) of *B. subtilis* cells. (h) G′ and G″ values of living materials comprising pAPBA-PEG$_{4k}$-pAPBA, pAPBA-PEG$_{10k}$-pAPBA, or pAPBA-PEG$_{20k}$-pAPBA with *B. subtilis* cells. (i) Optical image of hydrogels prepared by mixing pAPBA-PEG$_{4k}$-pAPBA with either WT *B. subtilis* (left) or engineered *B. subtilis* constitutively expressing RFP (right). Scale bars = 0.5 cm (j) Fluorescence image ($\lambda_{ex}$ = 630 nm, $\lambda_{obs}$ = 690–740 nm) of hydrogels prepared by mixing pAPBA-PEG$_{4k}$-pAPBA with either WT *B. subtilis* (left) or engineered *B. subtilis* constitutively expressing RFP (right). Scale bars = 0.5 cm. (k–l) Fluorescence image ($\lambda_{ex}$ = 630 nm, $\lambda_{obs}$ = 690–740 nm) of different shapes of hydrogels prepared by mixing pAPBA-PEG$_{4k}$-pAPBA with engineered *B. subtilis* constitutively expressing RFP. Scale bars = 1 cm.

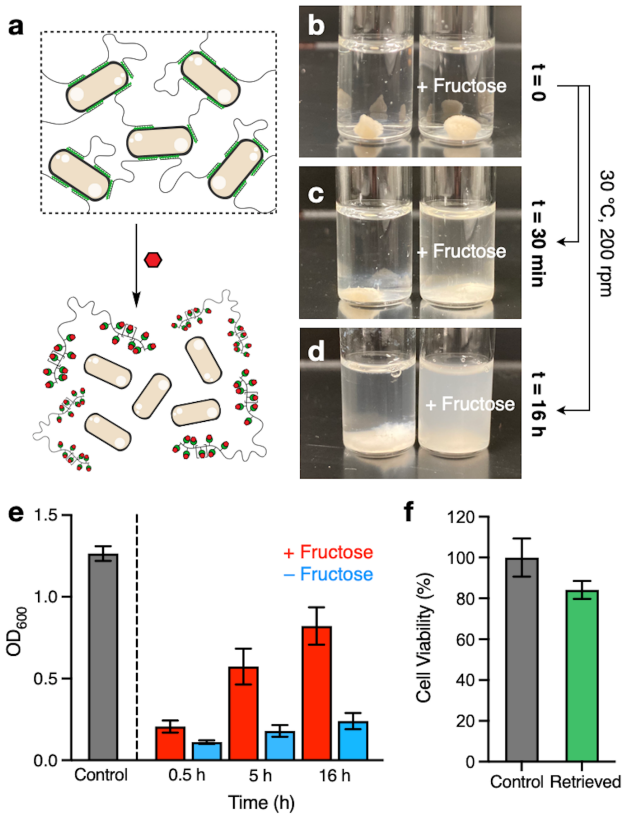


**Figure 5.** ***B. subtilis*** **cells encased in polymeric living material can be retrieved and analyzed upon exposure to competitive diol species.** (a) Schematic illustration of cell retrieval from living materials upon addition of competitive diol species. (b–d) Optical images of hydrogels immersed in PBS (20 mM, pH 7.4) in the absence (left) and presence (right) of fructose (100 mM). These immersed hydrogels were mechanically agitated (200 rpm) for 16 hours at 30 °C. (e) The absorbance at 600 nm ($OD_{600}$) of a supernatant from living materials immersed in PBS with fructose (red bar) and without fructose (blue bar). The control (gray bar) contains the same number of cells, based on $OD_{600}$, and is directly collected from the saturated bacterial cell culture. (f) Metabolic activities of retrieved cells (green bar) assessed by using 5-cyano-2,3-ditolyl tetrazolium chloride (CTC) reagent. The control contains the same number of cells, based on $OD_{600}$, and is directly collected from the saturated bacterial cell culture. $N = 3$ (biological replicates). Error bars represent ± s.e.m.

## ASSOCIATED CONTENT

### Supporting Information

The Supporting Information is available free of charge on the ACS Publications website.

## AUTHOR INFORMATION


### Corresponding Author

**Seunghyun Sim** – Department of Chemistry, Department of Biomedical Engineering, Department of Chemical and Biomolecular Engineering, University of California, Irvine, California 92697, United States.

Email: s.sim@uci.edu

### Author

**Hyuna Jo** –Department of Chemistry, University of California, Irvine, California 92697, United States.


## ACKNOWLEDGMENT


This work is supported by start-up funds from the University of California, Irvine. The authors also acknowledge the seed-funding support from the NSF Materials Research Science and Engineering Center (MRSEC), Center for Complex and Active Materials (CCAM) at the University of California, Irvine. The authors thank the Guan lab for use of their GPC, as well as Professor Guan for his helpful comments. Rheological measurements were performed at the Irvine Materials Research Institute Facility at the University of California, Irvine. Dynamic light scattering measurements were performed at the Laser Spectroscopy Labs, and the Nuclear Magnetic Resonance measurements were done in the NMR facility, both in the Department of Chemistry, University of California, Irvine.

**REFERENCE**


1. Marks Jr, S. C.; Popoff, S. N., Bone cell biology: the regulation of development, structure, and function in the skeleton. American Journal of Anatomy 1988, 183 (1), 1-44.
2. Errington, J., Regulation of endospore formation in Bacillus subtilis. Nature Reviews Microbiology 2003, 1 (2), 117-126.
3. González, L. M.; Mukhitov, N.; Voigt, C. A., Resilient living materials built by printing bacterial spores. Nature chemical biology 2020, 16 (2), 126-133.
4. Huang, J.; Liu, S.; Zhang, C.; Wang, X.; Pu, J.; Ba, F.; Xue, S.; Ye, H.; Zhao, T.; Li, K., Programmable and printable Bacillus subtilis biofilms as engineered living materials. Nature chemical biology 2019, 15 (1), 34-41.
5. Chakma, P.; Konkolewicz, D., Dynamic covalent bonds in polymeric materials. Angewandte Chemie 2019, 131 (29), 9784-9797.
6. Winne, J. M.; Leibler, L.; Du Prez, F. E., Dynamic covalent chemistry in polymer networks: A mechanistic perspective. Polymer Chemistry 2019, 10 (45), 6091-6108.
7. Marco-Dufort, B.; Iten, R.; Tibbitt, M. W., Linking molecular behavior to macroscopic properties in ideal dynamic covalent networks. Journal of the American Chemical Society 2020, 142 (36), 15371-15385.
8. Brooks, W. L.; Sumerlin, B. S., Synthesis and applications of boronic acid-containing polymers: from materials to medicine. Chemical reviews 2016, 116 (3), 1375-1397.
9. Deng, C. C.; Brooks, W. L.; Abboud, K. A.; Sumerlin, B. S., Boronic acid-based hydrogels undergo self-healing at neutral and acidic pH. ACS Macro Letters 2015, 4 (2), 220-224.
10. Smithmyer, M. E.; Deng, C. C.; Cassel, S. E.; LeValley, P. J.; Sumerlin, B. S.; Kloxin, A. M., Self-healing boronic acid-based hydrogels for 3D co-cultures. ACS macro letters 2018, 7 (9), 1105-1110.
11. Yesilyurt, V.; Webber, M. J.; Appel, E. A.; Godwin, C.; Langer, R.; Anderson, D. G., Injectable self-healing glucose-responsive hydrogels with pH-regulated mechanical properties. Advanced materials 2016, 28 (1), 86-91.

12. Cromwell, O. R.; Chung, J.; Guan, Z., Malleable and self-healing covalent polymer networks through tunable dynamic boronic ester bonds. Journal of the American Chemical Society 2015, 137 (20), 6492-6495.
13. Pasquina-Lemonche, L.; Burns, J.; Turner, R.; Kumar, S.; Tank, R.; Mullin, N.; Wilson, J.; Chakrabarti, B.; Bullough, P.; Foster, S., The architecture of the Gram-positive bacterial cell wall. Nature 2020, 582 (7811), 294-297.
14. Neuhaus, F. C.; Baddiley, J., A continuum of anionic charge: structures and functions of D-alanyl-teichoic acids in gram-positive bacteria. Microbiology and molecular biology reviews 2003, 67 (4), 686-723.
15. Allison, S. E.; D'Elia, M. A.; Arar, S.; Monteiro, M. A.; Brown, E. D., Studies of the genetics, function, and kinetic mechanism of TagE, the wall teichoic acid glycosyltransferase in Bacillus subtilis 168. Journal of Biological Chemistry 2011, 286 (27), 23708-23716.
16. Roy, D.; Cambre, J. N.; Sumerlin, B. S., Sugar-responsive block copolymers by direct RAFT polymerization of unprotected boronic acid monomers. Chemical Communications 2008, (21), 2477-2479.
17. Chang, C.-W.; Bays, E.; Tao, L.; Alconcel, S. N.; Maynard, H. D., Differences in cytotoxicity of poly (PEGA) s synthesized by reversible addition–fragmentation chain transfer polymerization. Chemical communications 2009, (24), 3580-3582.
18. Alexeev, V. L.; Sharma, A. C.; Goponenko, A. V.; Das, S.; Lednev, I. K.; Wilcox, C. S.; Finegold, D. N.; Asher, S. A., High ionic strength glucose-sensing photonic crystal. Analytical chemistry 2003, 75 (10), 2316-2323.
19. Cao, K.; Jiang, X.; Yan, S.; Zhang, L.; Wu, W., Phenylboronic acid modified silver nanoparticles for colorimetric dynamic analysis of glucose. Biosensors and Bioelectronics 2014, 52, 188-195.
20. Liu, Y.; Deng, C.; Tang, L.; Qin, A.; Hu, R.; Sun, J. Z.; Tang, B. Z., Specific detection of D-glucose by a tetraphenylethene-based fluorescent sensor. Journal of the American Chemical Society 2011, 133 (4), 660-663.
21. Pappin, B.; Kiefel, M. J.; Houston, T. A., Boron-carbohydrate interactions. Carbohydrates-comprehensive studies on glycobiology and glycotechnology 2012.

22. Angyal, S. J., The composition of reducing sugars in solution. In Advances in carbohydrate chemistry and biochemistry, Elsevier: 1984; Vol. 42, pp 15-68.
23. Angyal, S. J., The composition of reducing sugars in solution: Current aspects. Advances in carbohydrate chemistry and biochemistry 1991, 49, 19-35.
24. Brooks, W. L.; Deng, C. C.; Sumerlin, B. S., Structure–reactivity relationships in boronic acid–diol complexation. ACS omega 2018, 3 (12), 17863-17870.
25. Skarlatos, P.; Dahl, M. K., The glucose kinase of Bacillus subtilis. Journal of Bacteriology 1998, 180 (12), 3222-3226.
26. Blencke, H.-M.; Homuth, G.; Ludwig, H.; Mäder, U.; Hecker, M.; Stülke, J., Transcriptional profiling of gene expression in response to glucose in Bacillus subtilis: regulation of the central metabolic pathways. Metabolic engineering 2003, 5 (2), 133-149.
27. Olsen, B. D.; Kornfield, J. A.; Tirrell, D. A., Yielding behavior in injectable hydrogels from telechelic proteins. Macromolecules 2010, 43 (21), 9094-9099.

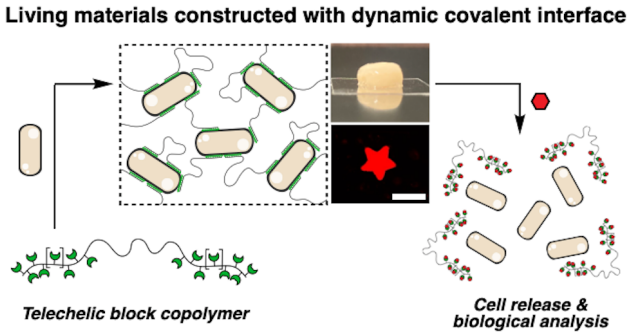


## Synopsis

This work reports living materials constructed via dynamic covalent bond formation between synthetic polymers and living bacterial cells. These materials allow reversible release of encased living cells for biological analyses.